Impact of Parylene-A Encapsulation on ZnO Nanobridge Sensors and Sensitivity Enhancement via Continuous Ultraviolet Illumination

C.-C. Huang, A.D. Mason, J.F. Conley, C. Heist, M.T. Koesdjojo, V.T. Remcho & T. Afentakis

Journal of Electronic Materials

ISSN 0361-5235
Volume 41
Number 5

Journal of Elec Materi (2012) 41:873-880
DOI 10.1007/s11664-011-1867-7

Springer

Journal of ELECTRONIC MATERIALS, Vol. 41, No. 5, 2012
DOI: 10.1007/s11664-011-1867-7

Impact of Parylene-A Encapsulation on ZnO Nanobridge Sensors and Sensitivity Enhancement via Continuous Ultraviolet Illumination

C.-C. HUANG,[1] A.D. MASON,[1] J.F. CONLEY JR.,[1,4] C. HEIST,[2] M.T. KOESDJOJO,[2] V.T. REMCHO,[2] and T. AFENTAKIS[3]

1.—School of Electrical and Computer Engineering, Oregon State University, Corvallis, OR 97331, USA. 2.—Department of Chemistry, Oregon State University, Corvallis, OR 97331, USA. 3.—Sharp Labs of America, Camas, WA 98607, USA. 4.—e-mail: jconley@eecs.oregonstate.edu

The impact of parylene-A encapsulation and the effect of continuous ultraviolet (UV) exposure on ZnO nanobridge sensor response are investigated. ZnO nanowire (NW) devices are fabricated using a novel method that involves selective growth of ZnO nanobridges between lithographically defined pads of carbonized photoresist (C-PR). We find that a thin coating of parylene-A effectively attenuates the response of NW devices to O_2, H_2O vapor, and UV illumination. The accessibility of the amine group on parylene-A for chemical functionalization is verified by transforming the amine groups on the surface of the parylene-A coating into aromatic imine groups, followed by UV–Vis absorption. Our results suggest that, in addition to modulating environmental sensitivity and providing protection of the ZnO NWs for liquid- and vapor-phase sensing, the parylene-A encapsulation may also serve as an activation layer for further specific functionalization targeting selective sensing. We also found that the sensitivity and response time of ZnO nanobridge devices to O_2 are dramatically improved by continuously exposing the nanobridge devices to UV illumination. Finally, we show that the C-PR directed growth method can also be used to isolate free-standing NW carpet.

Key words: ZnO, nanowire, parylene, CVD, nanobridge, sensor, functionalization, directed integration

INTRODUCTION

Two of the challenges in the application of nanowires (NWs) as biosensors are (i) integration of NWs into electrically accessible devices and (ii) functionalization for selective sensing.[1–13] Inspired by recent reports of selective growth of ZnO NWs on carbonized photoresist (C-PR),[14,15] we recently addressed the first challenge by using a lithographically patterned layer of C-PR[16,17] to direct the integration of ZnO nanobridge devices. This novel method of forming NW devices avoids the deposition and patterning of metal catalysts or seed layers as well as the use of silicon-on-insulator wafers. Growth and electrical connection of nanobridges take place simultaneously for devices across a substrate. We have shown previously that these ZnO nanobridge devices can operate as three-terminal devices, perform well as gas (O_2 and H_2O) sensors, and exhibit excellent sensitivity to ultraviolet (UV) exposure.[16,17] We have also recently addressed the second challenge by functionalizing the surface of ZnO nanobridge devices via adsorption of biotin.[18] However, the biotinylated ZnO nanobridges were found to dissolve rapidly in an aqueous environment. To protect the ZnO NW from moisture, we developed a chemical vapor deposition process for parylene-A. Parylene is a commonly used moisture barrier, and parylene-A has an amine functional group that should be available for modification or

(Received August 15, 2011; accepted December 9, 2011; published online December 29, 2011)

further functionalization. Previously, we demonstrated that parylene-A-coated ZnO NWs showed no signs of dissolution after 24 h in aqueous solution and that parylene-coated ZnO nanobridge devices were still functional as sensors.[18] However, the impact of parylene-A coating on the electrical performance of ZnO nanobridge devices and the possibility of further functionalization using the amine group were not fully investigated.

In this work we fabricated ZnO nanobridge devices using the C-PR method, investigated the impact of parylene-A coating on the UV and ambient sensitivity of ZnO nanobridge devices, and showed that the amine groups on parylene-A can be used for further functionalization. Since graphite (C-PR is composed primarily of graphite[14]) is known to exhibit a broad photoluminescence (PL)[19,20] which may obscure the actual ZnO PL signal, to provide more accurate PL measurement, we also report on the formation and characterization of free-standing NW carpet. The ZnO nanobridge devices investigated in this study incorporate several improvements in the device structure, layout, isolation, NW morphology, NW growth density, and cleaning that enhance the stability, repeatability, and sensitivity. We find that a thin coating of parylene-A increases device current and attenuates the response of devices to UV illumination, O_2, and H_2O vapor. As a demonstration that the amine groups on parylene-A are available for further functionalization, we estimate the surface amine density on parylene-coated glass samples using the UV–Vis techniques described by Moon et al.[21] Finally, we demonstrate that the sensitivity and response time of ZnO nanobridge sensors to O_2 are dramatically enhanced by continuous UV illumination. Our results suggest that, in addition to providing protection of the ZnO NWs for liquid- and vapor-phase sensing and modulating environmental sensitivity, encapsulation with parylene-A may also serve as an activation layer for further functionalization for selective sensing. Our results also show that continuous UV illumination may be used to increase sensor sensitivity and decrease response time.

EXPERIMENTAL PROCEDURES

Device Fabrication

ZnO nanobridge sensor devices were made on either (i) Si substrates with a 300-nm-thick steam-grown oxide as an insulating layer or (ii) insulating quartz substrates. The fabrication process is discussed in Ref. 17. Briefly, after deposition and direct photolithographic patterning of a layer of photoresist (Shipley 1818), the photoresist was carbonized at 900°C and 5 Torr for 60 min in a reducing atmosphere (95% Ar, 5% H_2).[14] Next, a 150-nm-thick layer of shadow mask-patterned molybdenum was sputtered from a 3-inch target at 100 W and pressure of 3.5 mTorr Ar. Vapor–solid growth of ZnO NWs was performed using ZnO (99.99%, Sigma-Aldrich) and graphite powders (99.9995%, Alpha Aesar) mixed in 1:1 ratio.[22] In this work, the ZnO/graphite mixture was vibratory milled (SWECO vibratory mill) in a bottle with ethanol using yttrium-stabilized zirconia media (Tosoh) for 6 h. The reason for using vibratory milling rather than hand mixing is to produce a uniform particle size, which enhances ZnO evaporation,[23] improves across-sample uniformity, improves run-to-run uniformity, and extends the range of growth parameters over which selective growth on C-PR is observed. Due to the wider growth temperature range (50°C versus 20°C) enabled by using vibratory milling, the NW diameter can be more effectively controlled. Following ethanol evaporation in an oven, the dry ZnO/graphite mixture was placed in a tube furnace at 920°C and 1.4 Torr with carrier gas flow of 150 sccm N_2 to carry the vapors downstream to the substrates at 770°C. O_2 gas at 1 sccm was introduced 5 cm upstream from the substrates to aid nanobridge growth. It was found that higher O_2 flow rates produced higher areal growth densities of NWs. Higher-density growth was in turn found to result in decreased sensor sensitivity. The decreased sensitivity observed for dense growth most likely can be attributed to increased probability of larger-diameter NWs (with lower sensitive surface-to-volume ratio) and increased shading, corresponding to a reduction in the UV intensity which can reach the underlying NWs near the substrate. The NW growth time used in this work was between 40 min and 2 h. Finally, an N_2 cleaning step, in which the sample is blown with N_2 for 1 min, was found to improve the stability and repeatability of the sensor response as well as reduce the recovery time between UV pulses. It is speculated that these improvements are due to removal of loose NWs or residual ZnO particulates.

Figure 1 shows (a) a schematic cross-section of the completed device structure and (b) a zoomed-in top-down scanning electron microscopy (SEM) image of part of one of the interdigitated fingers. In our previous work,[16–18] a simpler structure without interdigitated fingers was used. In this work, a string of serially connected interdigitated devices is also used, as shown in Fig. 1c. As discussed below, this serially connected device approach was found to improve repeatability and sensitivity.

Parylene Coating and Functionalization

The procedure for CVD coating of parylene-A is discussed more fully in Mason et al.[18] To summarize, in a single vacuum chamber amino-[2,2]paracyclophane (dix-A, Kisco) was vaporized at 150°C, pyrolized at 690°C, and then deposited on ZnO nanobridge devices held at room temperature. The parylene film thickness was adjusted by varying the amount of parylene-A dimer in the vaporization zone (unless otherwise indicated, 0.1 g was used).

Demonstration of the availability of the parylene-A surface amines was accomplished by following

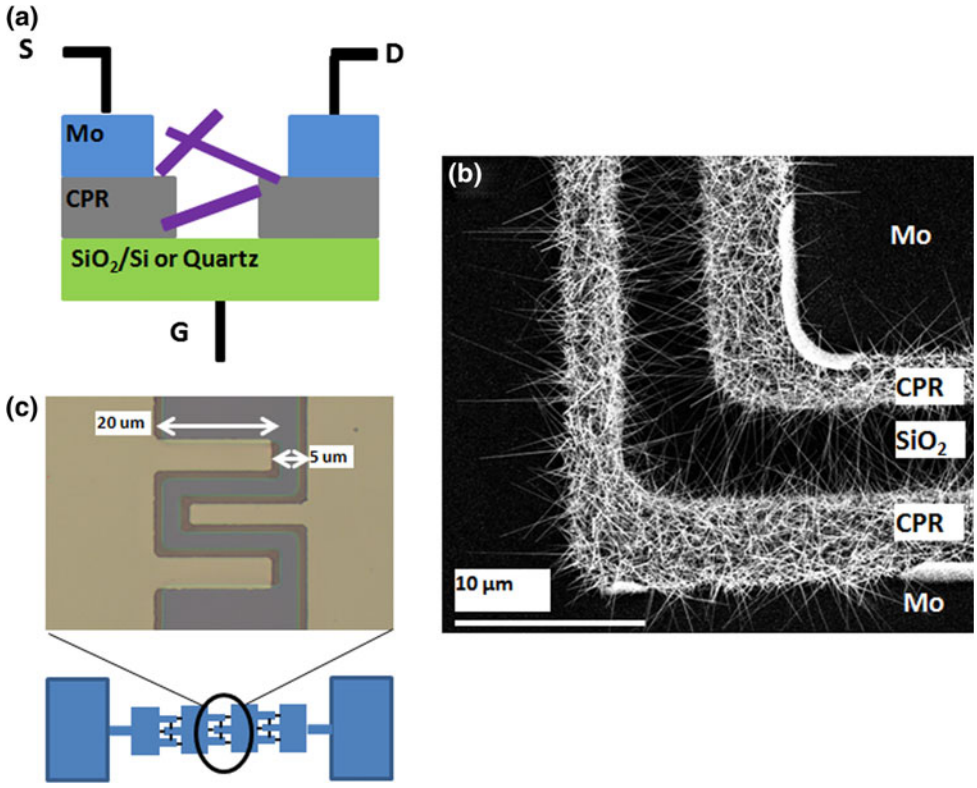

Fig. 1. (a) Schematic cross-section of the completed device structure and (b) zoomed top-down SEM image of the end of the middle interdigitated finger. As shown in (c), a string of serially connected interdigitated device structures is used.

the techniques of Moon et al.[21] The surface amine groups were transformed to aromatic imines by allowing the parylene-coated glass substrates to react with 2.6 mM 4-nitrobenzaldehyde [Fluka ≥99% in 0.08% acetic acid (0.02 mL acetic acid Fisher Scientific) in 25 mL absolute ethanol (Pharmoco-AAPER 200 proof)]. The reaction was performed under argon at 50°C for 3 h. The substrate was then washed with absolute ethanol and subsequently sonicated in absolute ethanol for 3 min before being dried under vacuum. The imines were then hydrolyzed in 0.2% acetic acid for a period of 1 h at 30°C. An aliquot of the resulting solution was then analyzed with UV–Vis (Agilent 8453).

Device Testing and Material Characterization

The *I–V* characteristics and UV response of parylene-coated and uncoated ZnO nanobridge devices were measured using a semiconductor parameter analyzer (Agilent 4155C) and a UV excitation source (Mineralight 254 nm, 18.4 W lamp). Measurements of the sensitivity of ZnO nanobridge devices to O_2 gas and H_2O vapor were performed using a semiconductor device analyzer (Agilent B1500) and a high-temperature measurement cell (NorECs ProboStat). Mass flow controllers (MFCs) were used to control gas flow rates. The concentration of H_2O was adjusted roughly by changing the ratio of flow rates for "wet" N_2 and dry N_2 at fixed total flow rate of 200 sccm. The wet N_2 was generated by flowing dry N_2 through a bubbler filled with deionized (DI) water at room temperature.

SEM imaging and energy-dispersive spectroscopy (EDS) were performed using an FEI Quanta at working distance of 10 mm and accelerating voltage of 20 kV. X-ray diffraction (XRD) was performed using a Bruker D8 Discover x-ray diffractometer with Cu K_α radiation. Room-temperature PL spectra were taken on an Accent Optical Technologies RPM200 equipped with an approximately 3.5 mW quadrupled Nd:YAG laser (266 nm) passed through a 295 nm low-pass filter. The luminescence was dispersed through a 600 g mm^{-1} grating blazed at 400 nm and detected by a back-thinned, thermoelectrically cooled charge-coupled device (CCD).

RESULTS

Formation of Nanowire Carpet and Nanowire Material Quality

Since the broad PL emission of graphite[19,20] (C-PR is primarily graphite) may obscure interpretation of the overlying ZnO NW PL results, free-standing NWs without C-PR attachment were needed for appropriate PL measurement. When the ZnO NW growth time is extended from 40 min to 2 h, a dense layer of ZnO NW "carpet" can be produced by the C-PR growth method, as shown in Fig. 2a. By rapidly cooling in air, the ZnO NW carpet can be

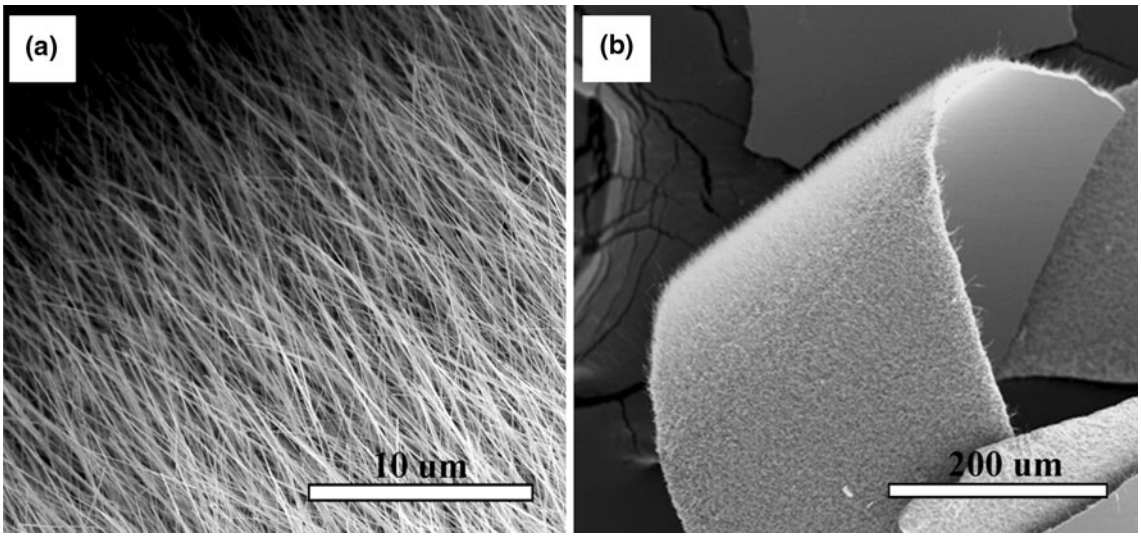

Fig. 2. SEM images of substrate-separated free-standing ZnO NW carpet.

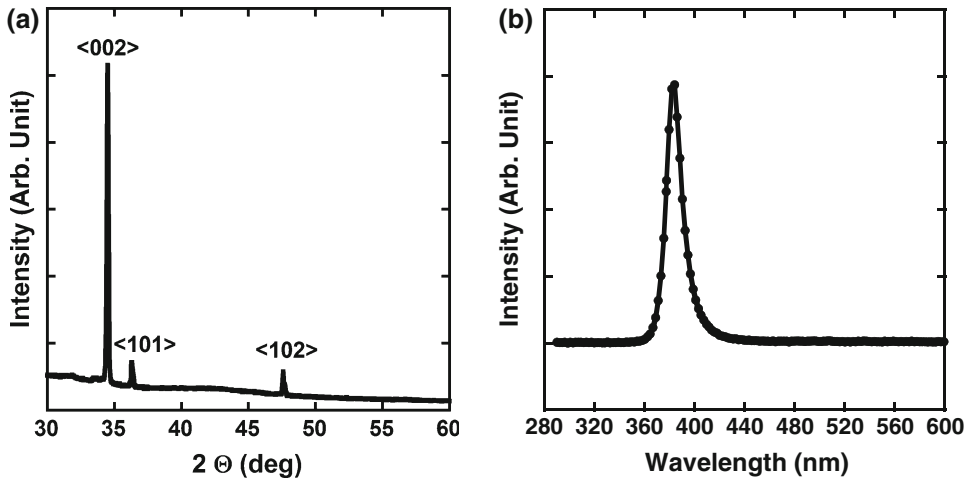

Fig. 3. (a) XRD intensity versus 2θ and (b) PL intensity versus wavelength for the ZnO NW carpet shown in Fig. 2.

separated from the substrate to form a free-standing structure as shown in Fig. 2b. Though the long growth conditions used to produce NW carpet are not desirable for sensor applications (we found that sparse NW growth produces sensors with higher sensitivity), free-standing NW carpet provided higher-resolution PL and XRD measurements. It is worth noting that no detectable carbon signal was observed on the back side of ZnO NW carpet using EDS. The free-standing NW carpet may also be useful for incorporation into a nano-piezo device structure that could be used for energy scavenging applications.[24–26]

To examine crystal quality, XRD measurements were performed and room-temperature PL spectra were taken on the ZnO NW carpet sample shown in Fig. 2. Figure 3a shows a plot of XRD intensity versus 2θ, indicating the hexagonal wurtzite phase of ZnO. The intense (002) peak indicates a *c*-axis preferred orientation. The plot of PL intensity versus wavelength in Fig. 3b reveals a strong emission peak at 380 nm due to an intrinsic near-band-edge recombination. No trace of emission is detected in either the green (broad peak centered around 510 nm) or orange (broad peak centered around 590 nm) regions, indicating a low density of oxygen vacancies and other defects.[27] The XRD results combined with the presence of a strong intrinsic UV PL peak and the absence of any defect-related/extrinsic visible PL evidence the high crystal quality of the NWs produced by the C-PR growth method.

Effect of Parylene Coating on Gas and UV Response

ZnO NW devices are known to be particularly sensitive to O_2 gas and H_2O vapor exposure. O_2

molecules can chemisorb on the ZnO NW surface, capturing an electron to become negatively charged and creating a surface depletion region that decreases conductivity.[28] H_2O molecules can interact with the ZnO NW surface and increase conductivity by either directly donating an electron or displacing a chemisorbed O_2 molecule. This sensitivity to ambient is not always desirable. We have shown previously that thin parylene-A encapsulation can protect ZnO NWs from dissolution in water.[18] Here, we directly compare the ambient and UV sensitivity of ZnO nanobridge devices before and after coating with parylene-A.

Figure 4 shows a comparison of the response to O_2 gas and H_2O vapor for serially connected 5-μm-gap nanobridge devices formed on a quartz insulating layer with V_{DS} = 3 V and V_G left floating, before (bare) and after coating with an approximately 20 nm thick layer of parylene-A (schematically illustrated in inset). Test gas flow rates of 50 sccm were used, with O_2 or H_2O flow switched on at 110 s. Measurements were made at room temperature. It is apparent that the magnitude of the response to both O_2 gas and H_2O vapor are attenuated by the parylene-A coating. The rate of response to both O_2 and H_2O is also reduced, suggesting that the parylene-A layer serves as a diffusion barrier.

ZnO NW-based devices are well known to be sensitive to UV light via two effects: (i) immediate direct photogeneration of charge carriers, and (ii) slower interaction with the ambient, in particular photoinduced desorption of O_2 from the NW surface.

Figure 5 shows a comparison of the UV response for serially connected 5 μm gap nanobridge devices fabricated on quartz with V_{DS} = 3 V before (bare) and after coating with an approximately 20-nm-thick layer of parylene-A. Measurements were performed at room temperature in air. Uncoated (bare), the devices have an $I_{D\text{-}UV}/I_{D\text{-}dark}$ ratio greater than 10^5 with very fast rise and fall times. Previously, we reported an $I_{D\text{-}UV}/I_{D\text{-}dark}$ ratio of up to 10^3 using nanobridge devices fabricated on SiO_2/Si substrates.[16] The 100× enhancement in UV response reported here is due to a number of improvements including the interdigitated device structure, the serial connection of several devices, isolation with a better insulating quartz substrate, small-diameter (~40 nm) NW morphology, sparser NW growth, and an N_2 cleaning step that together combine to reduce $I_{D\text{-}dark}$ and enhance stability, repeatability, and sensitivity.

After parylene coating, devices are found to have a higher $I_{D\text{-}UV}$. However, the $I_{D\text{-}dark}$ of the coated devices is increased by more than four orders of magnitude, leading to a net decrease in UV sensitivity. It is well established that a reduction in adsorbed O_2 reduces the depletion region at the NW surface and increases conductivity (see, for example, Ref. 28). The increase in both $I_{D\text{-}dark}$ and $I_{D\text{-}UV}$ after parylene-A coating could thus be due to desorption or displacement of surface-adsorbed O_2 or blocking of O_2 adsorption sites. The longer UV rise and fall times exhibited after coating are likely related to parylene-A acting as a diffusion barrier, decreasing the rate of O_2 adsorption and desorption from the ZnO NW surface. In fact, other types of

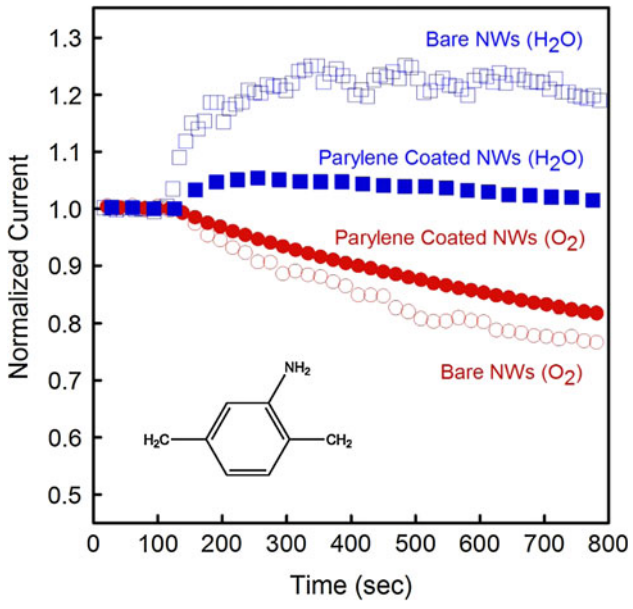

Fig. 4. Plot of normalized current (I_{D-O_2}/I_{D-N_2} or I_{D-H_2O}/I_{D-N_2}) versus time showing the O_2 (red circles) and H_2O (blue squares) response for serially connected NW devices before (open symbols) and after (solid symbols) parylene coating. The O_2 or H_2O gas flow is turned on at 110 s. Inset shows a parylene-A monomer (Color figure online).

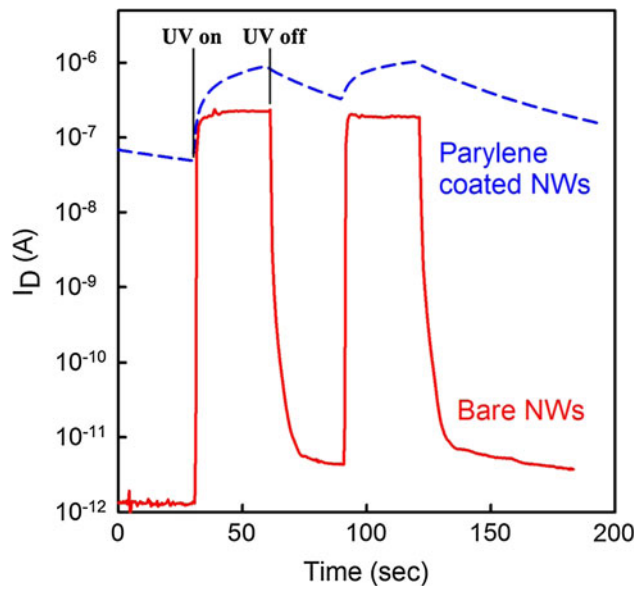

Fig. 5. Plot of log(I_D) versus time for 5-μm-gap serially connected nanobridge devices fabricated on a quartz substrate and exposed to 30-s periods of UV with V_{DS} = 3 V before (solid red) and after (dashed blue) parylene coating (Color figure online).

parylene find wide application as protective gas diffusion barriers. Note that other groups have reported enhanced UV sensitivity for polymer coatings such as polystyrene sulfate, which they propose is due to the polymer coating serving as a bridge for electron transfer to the ZnO NWs, analogous to the dye in dye-sensitized solar cells.[29]

Demonstration of Amine Group Modification

To demonstrate that the amine groups on the parylene-A encapsulating layer are accessible and modifiable, a 20 nm thick parylene-A film was coated on a glass substrate. Following the techniques of Moon et al.,[21] the non-UV-absorbing amine groups were exchanged for UV-absorbing imine groups. The reaction scheme is shown in Fig. 6a. The qualitative UV–Vis spectrum is shown in Fig. 6b, in which the positive absorbance at 281 nm indicates the presence of imines and therefore surface amines. This result demonstrates that the amine groups on the parylene-A coating are potentially useful for further functionalization and subsequent selective sensing.

Enhanced Gas Sensitivity via Continuous UV Exposure

Figure 7 shows comparisons between the O_2 response of 5 μm gap ZnO serially connected nanobridge devices on a quartz substrate in the dark and under continuous *in situ* UV illumination (a) before and (b) after parylene-A coating. Continuous *in situ* UV illumination was implemented by incorporating an InGaN light-emitting diode (LED) in the NorECs ProboStat. Prior to all measurements, a 2 h purge in 200 sccm N_2 was performed to achieve saturation of I_{D-N_2}. Devices were then subjected to 50 sccm O_2 flow at room temperature, and I_D was monitored at V_{DS} = 3 V with a floating back gate. Looking first at the uncoated device in Fig. 7a, it is seen that continuous UV exposure results in a dramatic increase in both the magnitude and speed of the response to O_2 exposure. The initial slopes for uncoated samples in the dark and under UV are approximately 0.0015 s^{-1} and approximately 0.04 s^{-1}, respectively. After 100 s of O_2 gas flow, the current drops by approximately 20% in the dark whereas an approximately 91% drop is observed when the

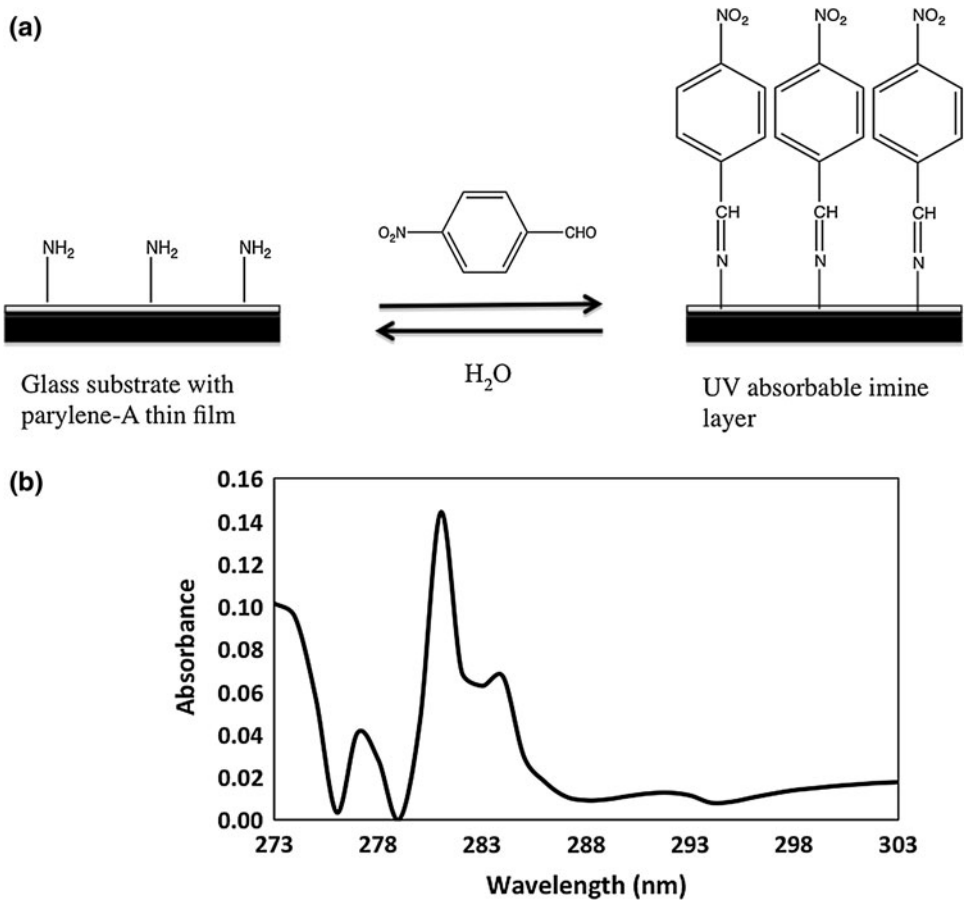

Fig. 6. (a) Reaction scheme illustrating the exchange of surface amines to aromatic imines with excess 4-nitrobenzaldehyde and recovery of the aminated layer via hydrolysis (adapted from Ref. 21), and (b) the portion of interest of the resulting qualitative UV–Vis spectrum (λ_{max} = 281 nm) used to confirm the presence of imines.

sample is under UV. A similar enhancement in magnitude and speed is seen after parylene-A coating in Fig. 7b. The initial slopes are $0.0004 \pm 0.00005\ s^{-1}$ in the dark and $0.009 \pm 0.001\ s^{-1}$ under UV. After 100 s, the current drops by approximately 3% to 4% in the dark while an approximately 68% drop in current is observed under UV. Finally, comparing the device response (a) before and (b) after coating, it is seen once again that the parylene-A coating reduces both the magnitude and speed of the response to O_2 exposure. Note, however, that the difference in the response to O_2 exposure between devices subjected to continuous UV illumination and devices left in the dark is actually larger for the coated devices.

DISCUSSION

The results presented in Fig. 4 demonstrate the ability of a parylene-A coating to modulate the environmental sensitivity of ZnO nanobridge devices. It is likely that increasing the thickness of the parylene-A layer would further attenuate both the O_2 and H_2O responses. However, there is a tradeoff. As demonstrated in Fig. 6, the primary reason for using parylene-A is that its amine group can be used as an attachment site for further functionalization. Specific detection of target analytes using this type of functionalization is dependent upon charge-based interaction with the ZnO surface. The thicker the parylene coating, the weaker this interaction is expected to be. Since both environmental sensitivity and analyte sensitivity are reduced with increasing coating thickness, there may be an optimum thickness of parylene-A coating for a given target analyte in a given measurement environment.

Note that parylene C has very recently been used to passivate and reduce the environmental sensitivity of carbon nanotube transistors (CNTs).[30] Although we have also found that parylene C is suitable for protection and environmental stabilization, the Cl group on parylene C is not as readily amenable to chemical modification as the amine group on parylene-A.

Elevated temperature has been widely used to improve the response speed of metal oxide sensors. It is clear from the data in Fig. 7 that continuous UV exposure can be used to further improve the sensitivity and response time of ZnO nanobridge sensors to O_2. As discussed above, UV illumination results in both creation of electron–hole pairs and desorption of adsorbed oxygen from the NW surface.[28] Whereas photoinduced charge carrier creation occurs almost instantaneously, desorption (as well as adsorption) of O_2 on the surface occurs on a much longer timescale. Under steady-state UV exposure, energy is available so that nonequilibrium concentrations of adsorbed O_2 are continuously removed from the surface, enabling the system to respond quickly to changes in the equilibrium O_2 concentration. It is very likely that continuous UV exposure can be used to enhance the sensitivity of ZnO nanobridge devices to other species as well.

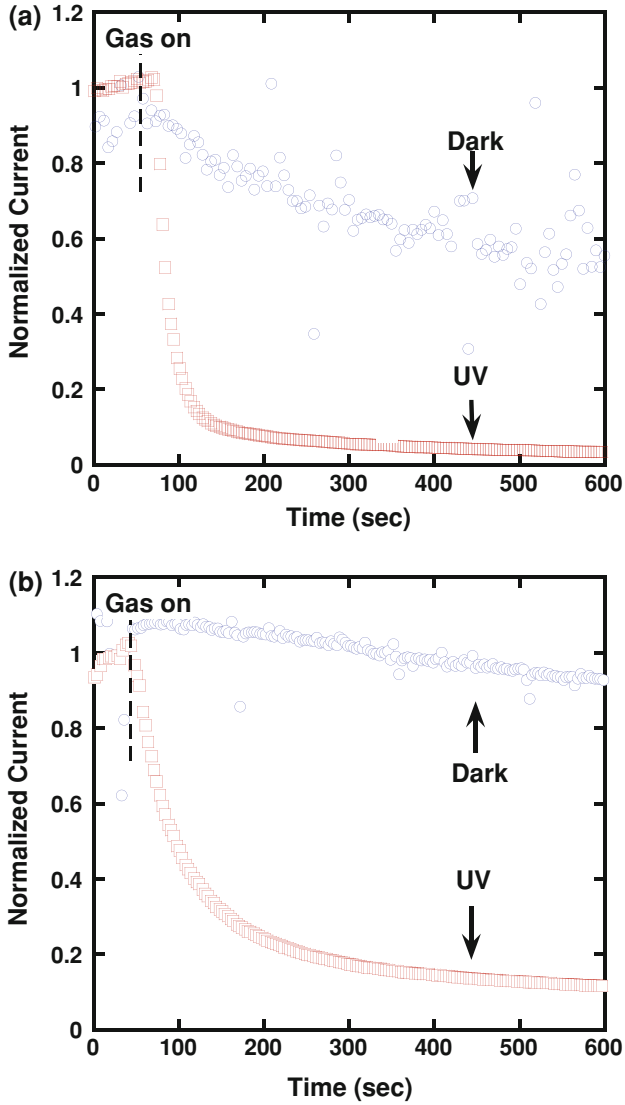

Fig. 7. Plot of O_2 response for 5-μm-gap serially connected nanobridge devices with V_{DS} = 3 V with (red squares) and without (blue circles) continuous *in situ* UV illumination (a) before and (b) after parylene-A coating (Color figure online).

CONCLUSIONS

We investigate the impact of parylene encapsulation and continuous UV exposure on ZnO NW sensors. We also report on the isolation of free-standing NW carpet. ZnO NW sensors were fabricated using a novel method that involves selective growth of ZnO nanobridges between lithographically defined pads of C-PR. We find that a thin coating of parylene-A attenuates the response of the ZnO NW devices to UV, O_2, and H_2O vapor. We also confirm that the amine groups on parylene-A coatings are accessible and that they can be chemically modified. Finally, we demonstrate that the O_2 response time and sensitivity are dramatically

improved by continuously exposing ZnO nanobridge devices to UV illumination.

Overall, we find that parylene-A encapsulation is a potentially viable method for surface protection and environmental stabilization of ZnO NW-based devices, as well as a platform for selective functionalization for specific analyte sensing. Our results also indicate that continuous UV illumination should be further investigated as a means for improving ZnO NW sensor sensitivity and response time for other analytes besides O_2.

ACKNOWLEDGEMENTS

The authors are grateful for the financial support provided by the Army Research Laboratory (W911NF-07-2-0083), the Office of Naval Research (N00014-07-1-0457), the Oregon Nanoscience and Microtechnologies Institute (ONAMI), the National Science Foundation (through an REU supplement to NSF DMR 0805372), and an Intel scholarship.

REFERENCES

1. Y. Cui, Q. Wei, H. Park, and C.M. Lieber, *Science* 293, 1289 (2001).
2. J.B.K. Law and J.T.L. Thong, *Nanotechnology* 19, 205502 (2008).
3. Y. Xia, P. Yang, Y. Sun, Y. Wu, B. Mayers, B. Gates, Y. Yin, F. Kim, and H. Yan, *Adv. Mater.* 15, 353 (2003).
4. M. Law, J. Goldberg, and P. Yang, *Annu. Rec. Mater. Res.* 34, 83 (2004).
5. E. Comini, *Anal. Chim. Acta* 568, 28 (2006).
6. N.S. Ramgir, Y. Yang, and M. Zacharias, *Small* 6, 1705 (2010).
7. M.-W. Ahn, K.S. Park, J.-H. Heo, D.-W. Kim, K.J. Choi, and J.-G. Park, *Sens. Actuators B* 138, 168 (2009).
8. Q. Wan, Q.H. Li, J. Chen, T.H. Wang, X.L. He, L.P. Li, and C.L. Lin, *Appl. Phys. Lett.* 84, 3654 (2004).
9. J.S. Wright, W. Lim, D.P. Norton, S.J. Pearton, F. Ren, J.L. Johnson, and A. Ural, *Semicond. Sci. Technol.* 25, 024002 (2010).
10. Y. Zeng, T. Zhang, M. Yuan, M. Kang, G. Lu, R. Wang, H. Fan, Y. He, and H. Yang, *Sens. Actuators B* 143, 93 (2009).
11. J.G. Lu, P. Chang, and Z. Fan, *Mater. Sci. Eng. R* 52, 49 (2006).
12. J.F. Conley Jr., L. Stecker, and Y. Ono, *Nanotechnology* 16, 292 (2005).
13. J.F. Conley Jr., L. Stecker, and Y. Ono, *Appl. Phys. Lett.* 87, 223114 (2005).
14. C. Cheng, M. Lei, L. Feng, T.L. Wong, K.M. Ho, K.K. Fung, M.M.T. Loy, D. Yu, and N. Wang, *ACS Nano* 3, 53 (2009).
15. P.G. Li, X. Wang, and W.H. Tang, *Mater. Lett.* 63, 718 (2009).
16. C.-C. Huang, B. Pelatt, and J.F. Conley Jr., *Nanotechnology* 21, 195307 (2010).
17. B. Pelatt, C.-C. Huang, and J.F. Conley Jr., *Solid State Electron.* 54, 1143 (2010).
18. A.D. Mason, C.-C. Huang, S. Kondo, M.T. Koesdjojo, Y.H. Tennico, V.T. Remcho, and J.F. Conley Jr., *Sens. Actuators B* 155, 245 (2011).
19. S.G. Yastrebov, V.I. Ivanov-OmskiĬ, and A. Richter, *Semiconductors* 37, 1165 (2003).
20. J.Q. Chen, J.A. Freitas Jr., and D.L. Meeker, *Diam. Relat. Mater.* 9, 48 (2000).
21. J.H. Moon, J.H. Kim, K.-J. Kim, T.-H. Kang, B. Kim, C.-H. Kim, J.H. Hahn, and J.W. Park, *Langmuir* 13, 4305 (1997).
22. M.H. Huang, Y. Wu, H. Feick, N. Tran, E. Weber, and P. Yang, *Adv. Mater.* 13, 113 (2001).
23. Z.L. Wang, *Mater. Sci. Eng. R* 64, 33 (2009).
24. Z.L. Wang, *Adv. Mater.* 19, 889 (2007).
25. Y. Gao, *Nano Lett.* 7, 2499 (2007).
26. K. Vanheusden, W.L. Warren, C.H. Seager, D.R. Tallant, J.A. Voigt, and B.E. Gnade, *J. Appl. Phys.* 79, 7983 (1996).
27. A.M. Glushenkov, H.Z. Zhang, J. Zou, G.Q. Lu, and Y. Chen, *Nanotechnology* 18, 175604 (2007).
28. Y.B. Li, V.F. Della, M. Simonnet, I. Yamada, and J.J. Delaunay, *Appl. Phys. Lett.* 94, 023110 (2009).
29. C.S. Lao, M.-C. Park, Q. Kuang, Y. Deng, A.K. Sood, D.L. Polla, and Z.L. Wang, *J. Am. Chem. Soc.* 129, 12096 (2007).
30. S. Selvarasah, A. Busnaina, and M.R. Dokmeci, *Appl. Phys. Lett.* 97, 153120 (2010).